A High-Repetition Rate LWFA for Studies of Laser Propagation and Electron Generation

Zhaohan He, James Easter, Bixue Hou, Karl Krushelnick, John Nees and Alec Thomas
Center for Ultrafast Optical Science, University of Michigan, Ann Arbor

Introduction

Advances in ultrafast optics today have enabled laser systems to deliver ever shorter and more intense pulses. When focused, such laser pulses can easily exceed relativistic intensities where the wakefield created by the strong laser electric field can be used to accelerate electrons (see Fig. 1). Laser wakefield acceleration (LWFA) of electrons holds promise for future compact electron accelerators or drivers of other radiation sources in many scientific, medical and engineering applications. Here we present preliminary experimental results of laser wakefield acceleration using the λ-cubed laser at the University of Michigan -- a table-top high power laser system operating at 500 Hz repetition rate. The high repetition rate allows statistical studies of laser propagation and electron acceleration which are not accessible with typical sub-0.1 Hz repetition rate systems from all previous LWFA experiments using large laser facilities. In addition, we carry out computational particle-in-cell simulations using the code OSIRIS to study the interactions.

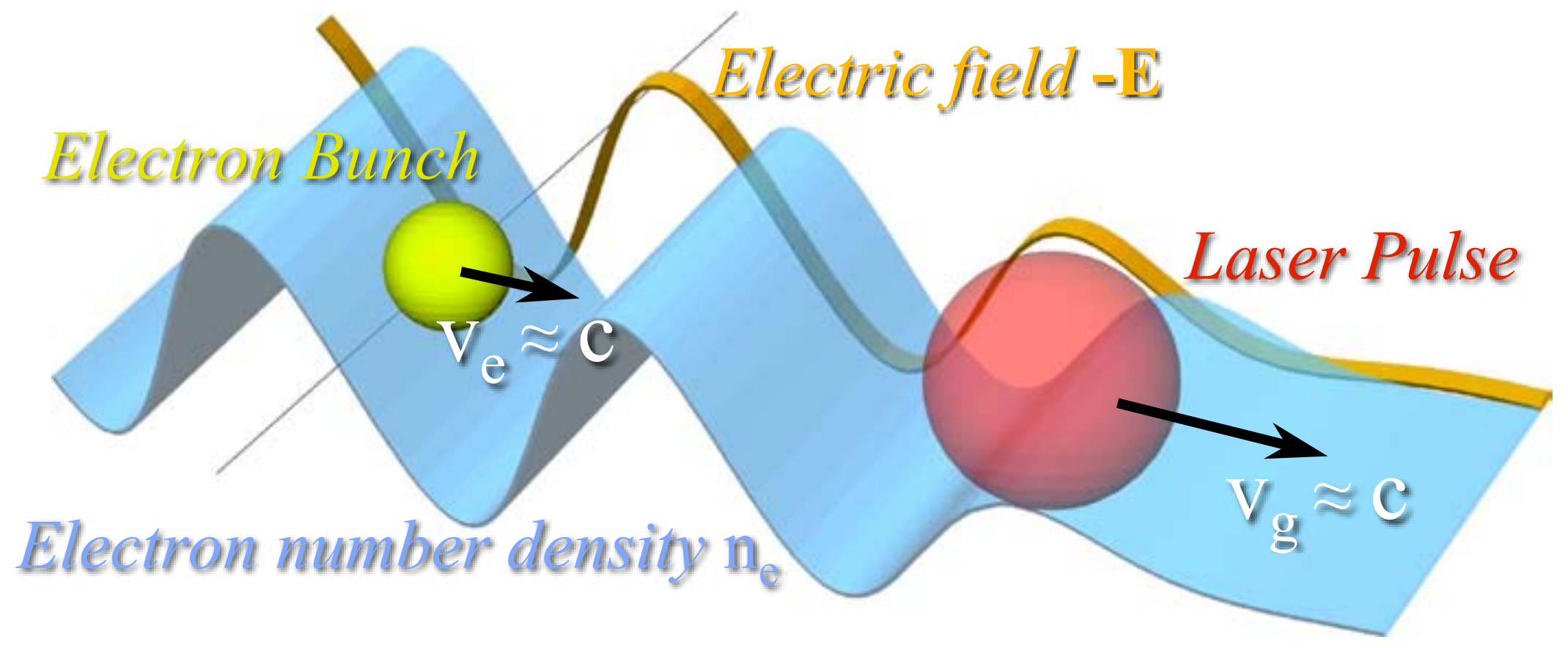

Fig. 1. Schematic of LWFA. A focused ultra short intense laser pulse excites large amplitude plasma waves as it propagates in underdense density plasma. The plasma waves have phase velocities close to the speed of light, which provide a high gradient electric field to accelerate electrons to relativistic energies.

Experimental Setup and Results

Charaterization of gas density profile using the Mach-Zehnder interferometer

The gas nozzle design is important to create desired gas density profile suitable for laser plasma interaction. Supersonic nozzles of millimeter size are commonly used to provide a uniform plateau profile with sharp edges in LWFA experiments where the focused power laser power is at least two magnitudes higher than in our experiments. However, such a supersonic gas source is not readily accessible with dimensions of about a hundred micrometers required in our experiments. As a result, fused silica capillary tubing is employed as our gas targets. In absence of any supersonic nozzle designs, the gas jet experiences free expansion from a high-pressure capillary tube into vacuum. Interferometric characterization was performed using argon gas at different backing pressures and tubing lengths under continuous gas flow.

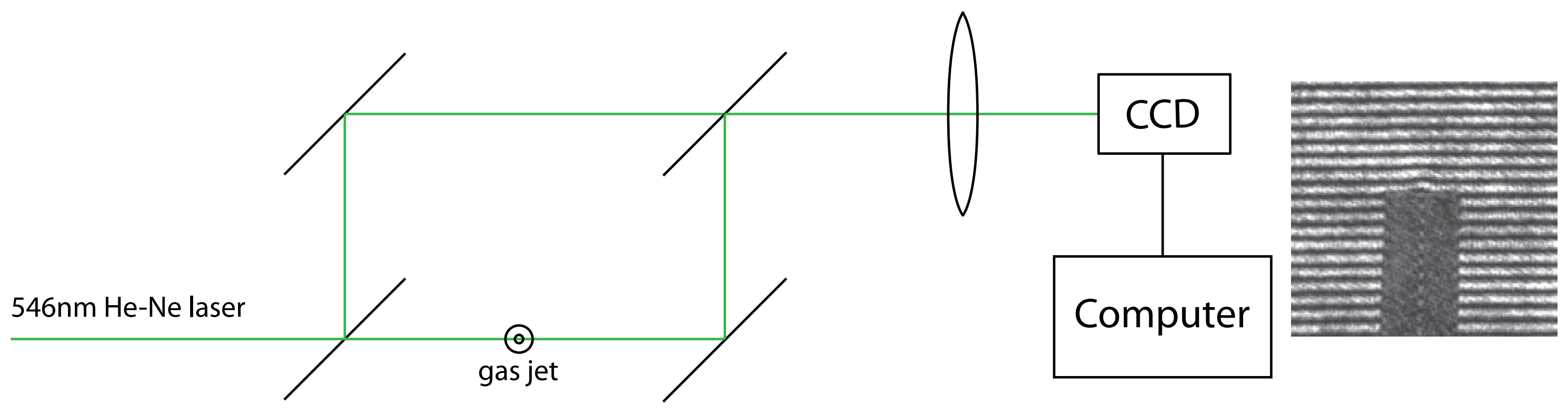

(a) (b)

Fig. 2. (a) Experimental setup for characterization of the gas jet using Mach-Zehnder interferometer (b) Spectrogram data

The experimental configuration is shown in Fig. 2(a). Assuming the cylindrical symmetry, the three-dimensional gas density profile can be obtained by applying Abel inversion to the interferogram data (Fig. 2(b)). The results indicate that the gas jet has an approximate Gaussian density transversely and it diverges quickly at longer distances away from tube exit (Fig. 3). Due to the fact that helium has a refractive index of 1.000035 which, compared to argon of 1.00028, is too small to cause any observable fringe shift even with the highest reachable pressure, we were unable to characterize helium gas jet by this approach. As a matter of fact, the phase shift created by argon at lower pressures again fails to yield any measurable signals above the noise level. Therefore, presently we can only extrapolate for the range of needed backing pressure of helium gas used in our LWFA experiments.

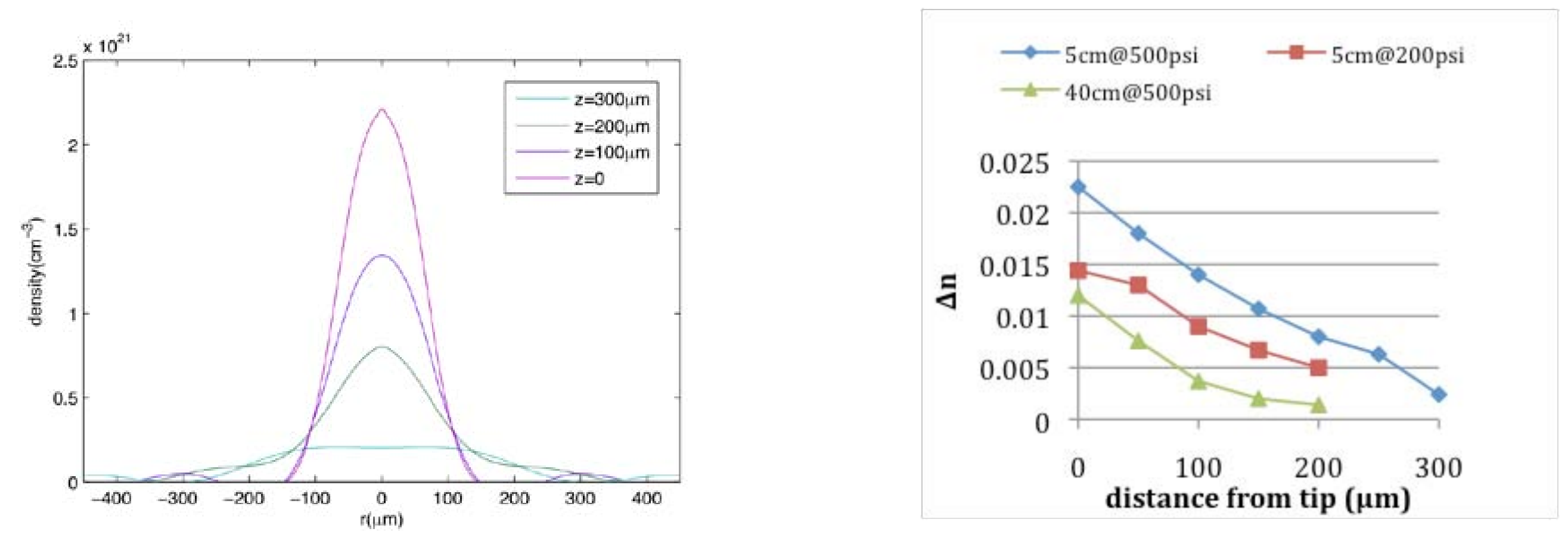

Fig. 3. Spatial density profile characterization of Argon. The left graph is the transverse density distribution at different distances from the tip. The right graph is the change of refractive index (proportional to denstiy) caused by the gas at distances at different backing pressures and tubing lengths from the center of the tip.

Laser wakefield acceleration experiment

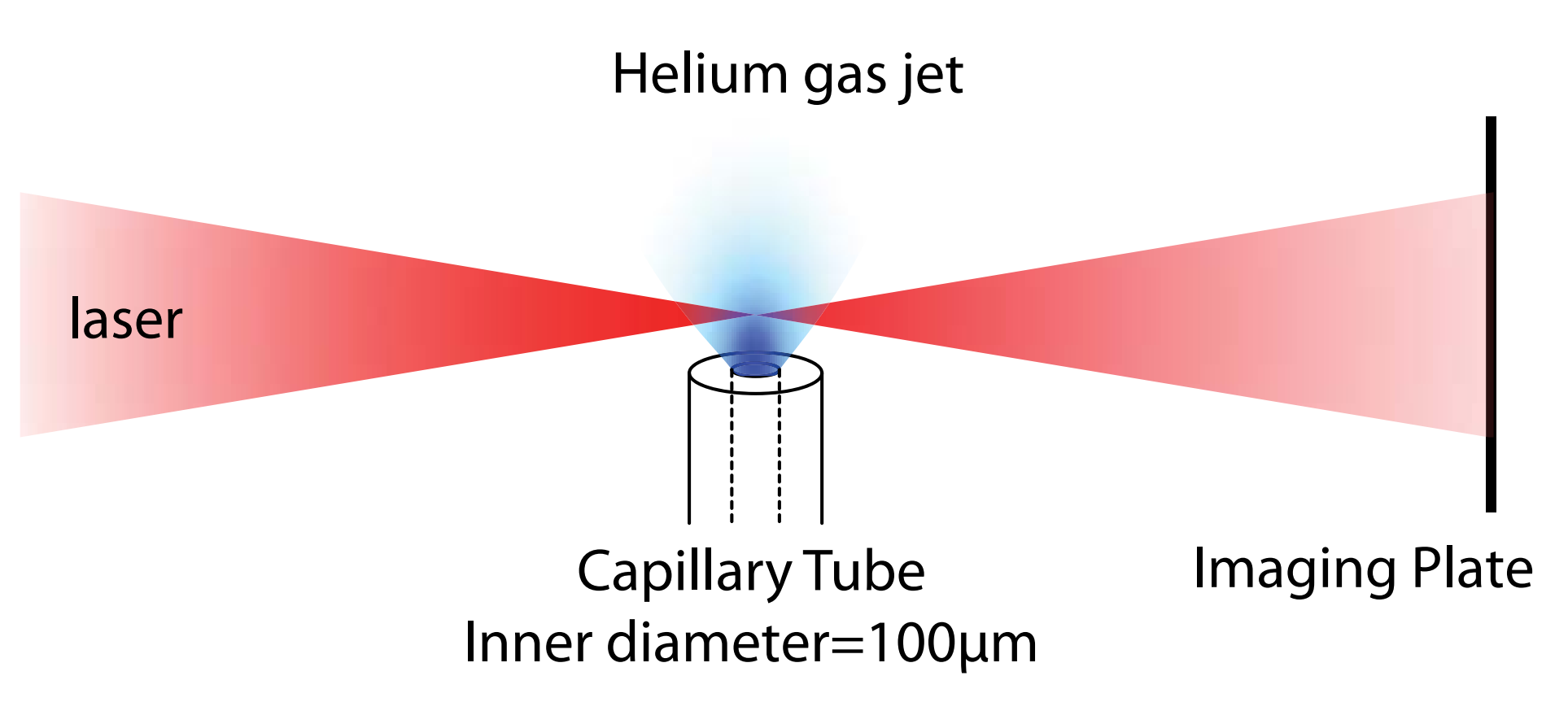

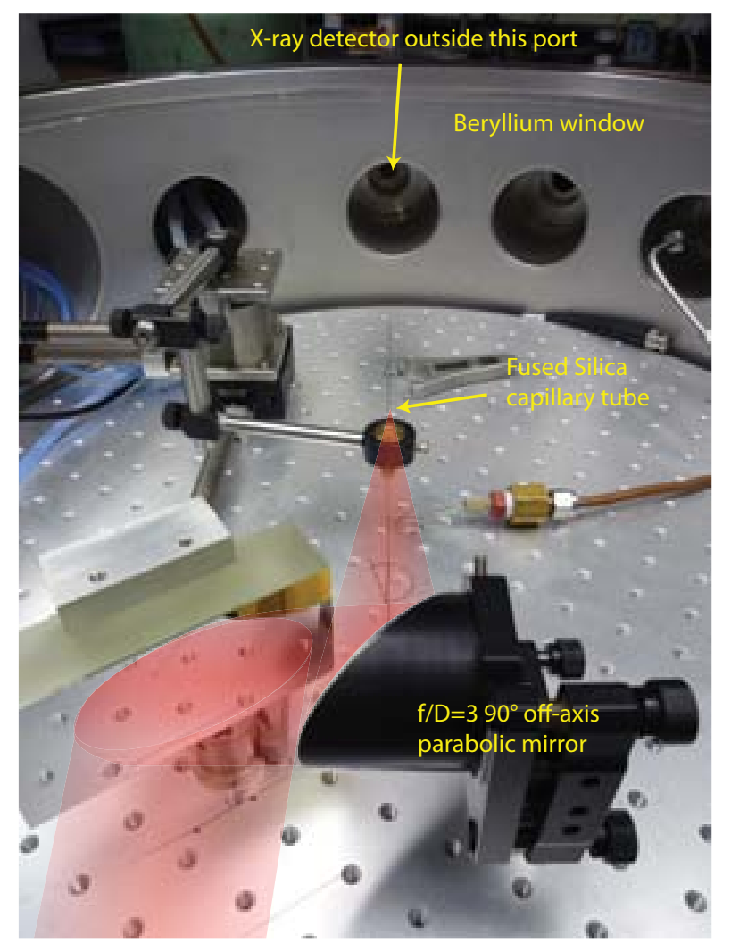

Fig. 4. Experimental configuration of LWFA. On the right, a picture of the apparatus is shown.

The experimental setup is shown in Fig. 4. The Lambda Cubed laser system at the University of Michigan Center for Ultrafast Optical Science is capable of delivering 10mJ femtosecond pulses at a repetition rate of 500Hz. The laser beam is focused by a f/3 off-axis parabolic mirror to a spot size of about 3μm, yielding a peak intensity exceeding the relativistic threshold about 10^{18}W/cm^2. The gas target is controlled by a motorized manipulator on a xyz translation stage, which allows micron accuracy operation. A CdTe X-ray detector is used outside the vacuum chamber providing online diagnostic information to facilitate the optimization of gas target position and gas pressure. Electrons generated by the plasma will travel through the beryllium vacuum window into the detector. The detector is connected to the oscilloscope for a live signal trace and the PC for count rate and spectrum measurements. For electron detection, imaging plates (Fuji BAS-SR) are used after the target. Electron beams with divergence of ~5° have been observed in these experiments (Fig. 5). The photo-stimulated luminescence (PSL) value obtained from the IP data is proportional to the amount of electron it has been exposed to. A rough calibration for our type of IP can be done by the relation 1 PSL = 50 electrons to estimate the beam charge. It is found that electron signal can be quite sensitive to the gas target position, which governs the laser focus with respect to the plasma (along laser propagation axis) and the plasma length (height of capillary tubing end).

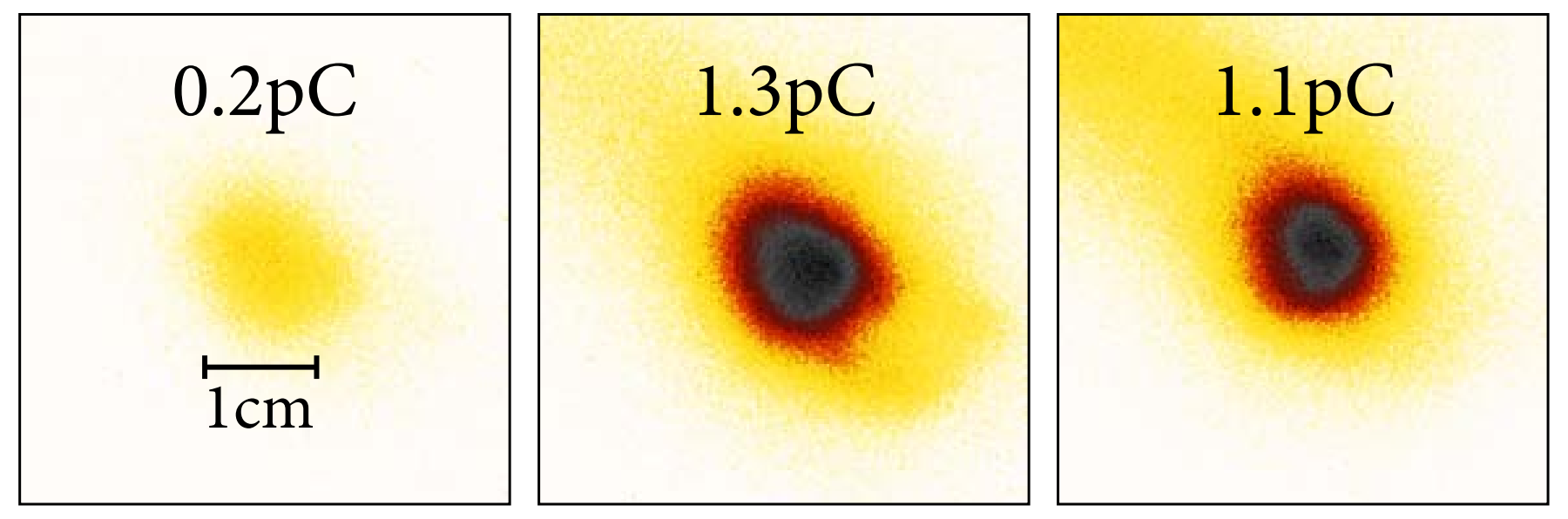

Fig. 5. (on the left) IP data for electron detection (false color is applied). The IP was placed at ~12cm behind the target. About 30000 laser pulses (one minute exposure time) were fired. The gas target was at three different positions separated by 40μm along the laser propagation axis.

Computational Simulations

Particle-in-cell simulations were performed to study laser wakefield acceleration for our experiments using the 2D3P relativistic PIC code OSIRIS. The simulation space is 900×1200 grid cells (30 cells per laser wavelength) with 2 electrons per cell in each dimension. The simulation box is moving at the speed of light. The laser pulse has 10mJ energy and the focal spot size is 3μm. The pulse duration is specified by a rise time and a fall time that have an approximate Gaussian shape, with parameters translating to a FWHM 25fs pulse. It is assumed the laser is sufficiently intense so that its electric field will instantaneously rip off the electrons of the gas molecules to form fully ionized plasma. Ions are considered to be immobile and merely treated as a neutralizing background. Therefore, only one species (i.e. electron) is implemented. The initial electron density profile assumes a Gaussian shape in the laser propagation direction to simulate our capillary gas target. The transverse density profile is uniform, which is a valid approximation because the transverse dimension in our simulation domain is small compared to the gas scale length.

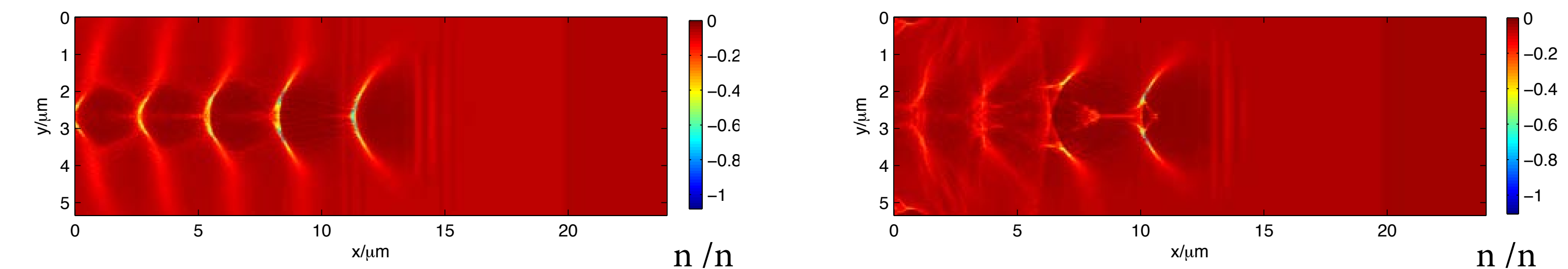

(a) t=350fs (b) t=400fs

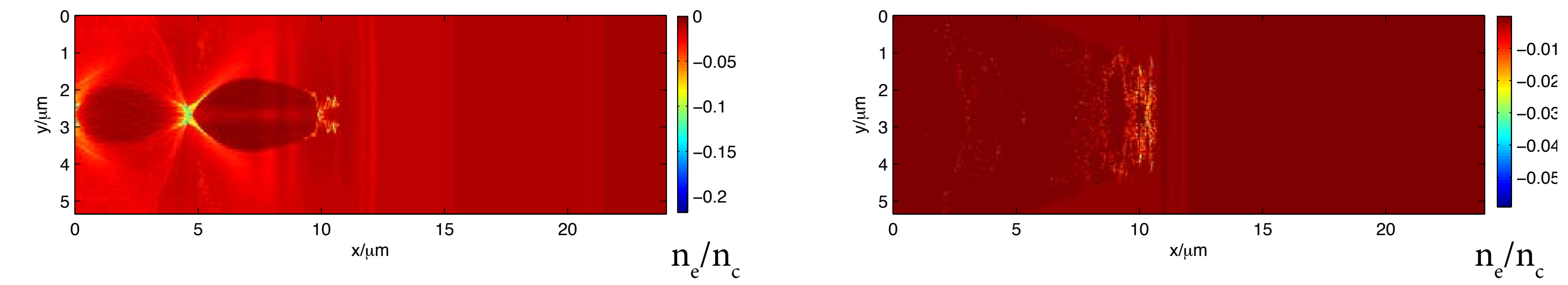

(c) t=550fs (d) t=720fs

Fig. 6. Electron density evolution snap shots. (x coordinates in moving frame)

In Fig. 6, a sequence of electron density snap shots reveals the interaction structure evolution. (a) The laser excites a plasma wakefield as the pulse propagates; (b) electrons are expelled outward by ponderomotive force and some electrons are injected into the cavitated regions of plasma waves as being accelerated to relativistic energies; (c) The laser pulse erodes and diffracts and the electron bunch spread out as they outrun the laser pulse; (d) the electrons travelling out of the plasma after the laser is depleted. For an effective laser plasma accelerator, the bunched electrons need to be extracted before they reach de-phasing distance and consequently are de-accelerated. By varying the Gaussian width of the density profile, it is found in these simulations that the accelerated electrons can leave the plasma when the full width half maximum of the Gaussian density profile is about 100μm, which matches our choice of capillary tubing as the gas target.

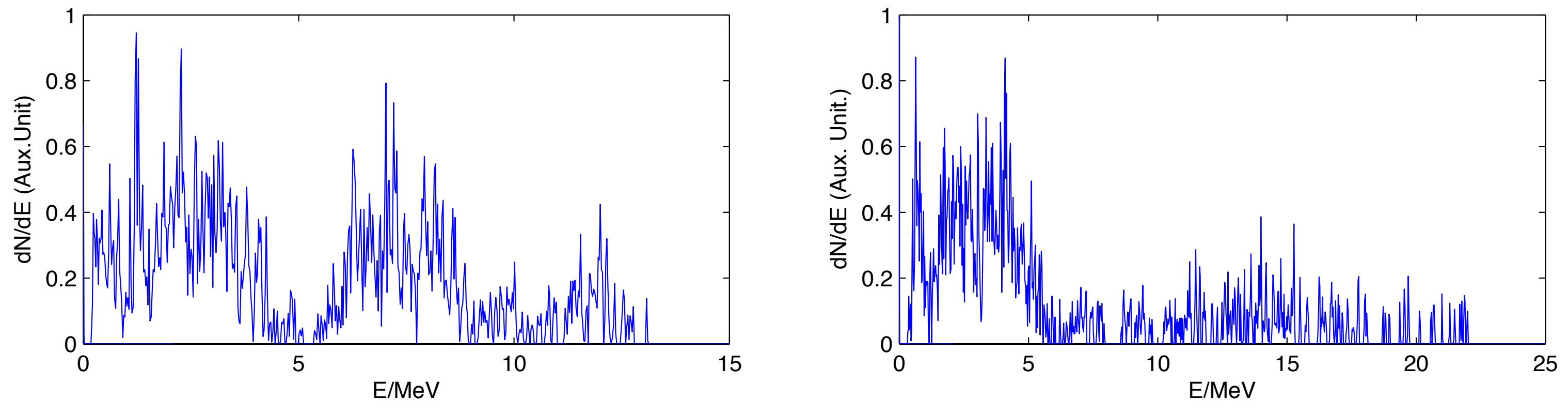

(a) (b)

Fig. 7. Two distinct spectra from LWFA simulations: (a) laser focus is 100μm before the gas density peak. (b) laser focus is 50μm before the gas density peak. Higher energy electrons up to 20MeV are produced with a broad spectrum.

Our simulations also reveal that the position of the laser focus with respect to the plasma can have an effect on the generated electron beam in their energy, charge and divergence. Two typical electron spectra are shown in Fig. 7. The optimization of LWFA performance for such a non-uniform density plasma interaction with laser can be very complicated. We expect to gain some insight via the computational simulations. A general expression for the de-phasing distance can be written as $L_d=2\pi c\omega_L^2/\omega_p^3$, where $\omega_p=(n_e e^2/\varepsilon_0 m_e)^{1/2}$ is the plasma frequency. In our situation, the non-uniformity of plasma density causes electrons to experience a varying dephasing distance. One of the consequences in this complex process is that trapped electrons in the first two or three cavities behind the laser pulse have different behaviors as visualized from the simulations. These electrons can be accelerated to different energies and may exhibit a multi-peaked quasi-monoenergetic distribution (see Fig. 7(a)). Under other conditions, electrons with higher energies can also be generated in our computational experiments (see Fig. 7(b)).

Conclusion

In conclusion, we have presented results of preliminary experiments and computational simulations for laser wake field acceleration using a high-repetition rate, milijoule pulse energy laser system. Experimentally, electron beams have been observed by using the imaging plates. Numerical studies show quasi-monoenergetic electrons up to 10MeV can be generated under certain conditions. Future experiments include: (1) using the electron spectrometer to measure the electron spectra from experiments; (2) developing techniques to optimize the laser focus quality using a deformable mirror; (3) using interferometric characterization to measure the actual plasma density at various delay times. On the computational side, a full three-dimensional simulation with ionization effect will be implemented in the future to provide a more accurate picture of the physical phenomena.